

Low-temperature heat capacity and thermochemical study of crystalline $[Y_2(Ala)_4(H_2O)_8](ClO_4)_6$ ($Ala=CH_3CH(NH_3^+)COO^-$)

Beiping Liu^{a,b}, Xinsheng Zhao^a, Lin Li^b, Lixian Sun^a, Zhi-Cheng Tan^{a,*}

^aThermochemistry Laboratory, Dalian Institute of Chemical Physics, Chinese Academy of Sciences, Dalian 116023, PR China

^bDepartment of Chemistry, Changde Normal College, Changde 415000, PR China

Received 4 January 2002; received in revised form 11 January 2002; accepted 31 January 2002

Abstract

The solid complex of rare-earth compound with alanine, $[Y_2(Ala)_4(H_2O)_8](ClO_4)_6$ were synthesized, and the heat capacities of the solid complex were measured with a small sample high-precision automated adiabatic calorimeter over the temperature range from 78 to 400 K. The melting point, molar enthalpy and entropy of fusion of the complex were determined to be 378.73 ± 0.01 K, 16.78 ± 0.02 kJ mol⁻¹, 44.30 ± 0.04 JK⁻¹ mol⁻¹, respectively. Thermal decomposition of the complex was studied through differential scanning calorimetry (DSC) and thermogravimetry (TG). The possible mechanisms of the thermal decomposition reaction was suggested according to the TG and DSC results. © 2002 Elsevier Science B.V. All rights reserved.

Keywords: $[Y_2(Ala)_4(H_2O)_8](ClO_4)_6$ (Ala = alanine); Heat capacity; Adiabatic calorimetry; TG analysis; DSC analysis

1. Introduction

The complexes of rare-earth compounds with α -alanine were extensively studied in the last two decades [1–6] due to their important role in living systems, dying industry and agriculture. The crystal structures of these complexes have been studied. However, the low-temperature heat capacities and thermodynamic properties of these complexes have been scarcely reported in literature.

The single crystal of rare-earth metal perchlorates with DL-Ala have been synthesized, their crystal structures and crystal parameter have been measured.

In order to improve the process of chemical synthesis of these substances and to perform relevant application and theoretical research, their thermodynamic data are in urgent needs both in rare-earth science and technology.

Since heat capacity is a basic quantity for evaluation of thermodynamic properties, heat capacity measurements of the complex were carried out in the temperature range between 78 and 400 K with a small sample automated adiabatic calorimeter. The melting temperature, the molar enthalpy and entropy of fusion of the complex were determined on the basis of heat capacity measurements. In addition, the thermal decomposition of the complex were studied by thermogravimetry (TG) and differential scanning calorimetry (DSC), respectively. A possible mechanism of the decomposition reaction was deduced according to the TG and DSC analysis.

* Corresponding author. Tel.: +86-411-4379215;

fax: +86-411-4691570.

E-mail address: tzc@dicp.ac.cn (Z.-C. Tan).

2. Experimental

2.1. Sample preparation and characterization

The titled complex was prepared by reaction of corresponding $Y(\text{ClO}_4)_3$ and DL-Ala with mole ratio 1:2 in aqueous solution at $\text{pH} = 4.0$. The mixed solution was stirred in the $80\text{ }^\circ\text{C}$ water bath for 6 h. The mixed solution was concentrated by evaporation. Afterwards, the solution was cooled and filtered. The filtrate was kept in desiccator with P_2O_5 until crystalline products were separated out from the solution. The crystals were filtered out and washed with absolute alcohol. Finally, the collected crystals were desiccated in a dryer to prevent the complex from deliquescent in air.

The actual content of the rare-earth metal ion obtained by EDTA titrimetric analysis was very close to the theoretic content of rare-earth metal ion in the sample. The results of EDTA titrimetric analysis demonstrated that the purity of the sample is higher than 99.70%, which is good enough to meet the requirement of the calorimetric study.

2.2. Adiabatic calorimetry

The heat capacity measurements were performed by means of a high-precision automatic calorimeter over the temperature range from 78 to 400 K. The principle and structure of the adiabatic calorimeter were described in detail elsewhere [7]. Briefly, the calorimeter mainly comprises a sample cell, a platinum resistance thermometer, an electric heater, an inner and an outer adiabatic shields, two sets of chromel–copel (Ni 55%, Cu 45%) thermocouples and a vacuum can. The sample cell was made of gold-plated copper and had an inner volume of 6 cm^3 . Four gold-plated copper vanes of 0.2 mm thickness were put into the cell to promote heat distribution between the sample and the cell. The platinum resistance thermometer was inserted into the copper sheath which was soldered at the bottom of the sample cell. The heater wire was wound on the side surface of the cell. The lid of the cell with a copper capillary was sealed to the sample cell with adhesive after the sample was loaded in it. The air in the cell was evacuated and a small amount of helium gas (0.1 Mpa) was introduced into it to enhance the heat transfer within the cell. The capillary was pinched off and soldered with a little

amount of solder. In order to obtain good adiabatic conditions between the calorimeter cell and its surroundings, the temperature difference between them was kept to be 0.5 mK during the whole experimental process. The temperature differences between the sample cell and the inner shield, and between the inner and outer shields were monitored by two sets of six junction chromel–copel (Ni 55%, Cu 45%) thermocouples, and controlled by two sets of DWT-702 precision temperature controller (manufactured by Shanghai NO. 6 Automated Instrumentation works). The vacuum can was evacuated to eliminate heat convection. The electrical energy introduced into the sample cell and the equilibrium temperature of the cell, after the energy input were automatically picked up by use of the Data Acquisition/Switch Unit (Model 34970A, Agilent, USA), and processed on line by a computer.

To verify the accuracy of the calorimeter, the heat capacity measurements of the reference standard material, $\alpha\text{-Al}_2\text{O}_3$ were made. The deviations of our experimental results from the recommended values reported by Ditmas et al.[8] of the National Bureau of Standards lie within $\pm 0.2\%$, in the entire experimental temperature range.

2.3. Thermal analysis

A thermogravimetric analyzer (Model TGA/SDTA 851e, METTLER TOLEDO, Switzerland) was used for TG measurements of the solid complex in nitrogen atmosphere. The mass of the sample used for TG analysis was 1.7688 mg, and the heating rate was $10\text{ }^\circ\text{C min}^{-1}$.

A DSC (Model: 910s, TA) was used to perform the thermal analysis of $[\text{Y}_2(\text{Ala})_4(\text{H}_2\text{O})_8](\text{ClO}_4)_6$ solid complex. The mass of the sample used for DSC analysis was 6.9190 mg, with a heating rate of $50\text{ }^\circ\text{C min}^{-1}$. The atmosphere was nitrogen gas with purity of 99.999%, and a flow rate of 100 ml min^{-1} .

3. Results and discussion

3.1. Heat capacity

The low-temperature experimental molar heat capacities of $[\text{Y}_2(\text{Ala})_4(\text{H}_2\text{O})_8](\text{ClO}_4)_6$ solid complex are shown in Fig. 1 and listed in Table 1, respectively.

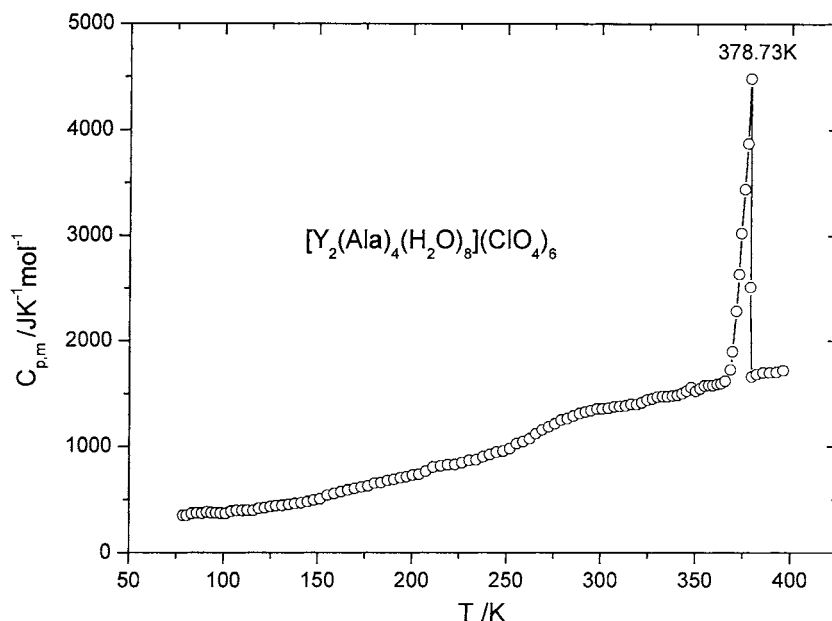


Fig. 1. Experimental heat capacity curve of $[\text{Y}_2(\text{Ala})_4(\text{H}_2\text{O})_8](\text{ClO}_4)_6$ as a function of temperature.

From Fig. 1, it can be seen that the heat capacities of the complex increase with increasing temperature in a smooth and continuous manner in the temperature range from 78 to 368 K, which implies that the complex is stable in the above temperature range. However, a solid to liquid phase transition was observed in the range of 368–378 K with a peak temperature of 378.13 ± 0.01 K. The experimental molar heat capacities have been fitted to the following polynomials in reduced temperature (X) by means of the least square fitting.

For the solid phase over the temperature range from 78 to 364 K:

$$\begin{aligned} C_{p,m}(\text{J K}^{-1} \text{mol}^{-1}) &= 842.0759 + 836.6935X + 245.8627X^2 \\ &+ 244.7354X^3 - 126.8897X^4 - 19.5857X^5 \quad (1) \end{aligned}$$

where $X = (T - 221)/143$, T is the absolute temperature. The correlation coefficient of the fitted curve, $R^2 = 0.9972$.

For the liquid phase:

$$\begin{aligned} C_{p,m}(\text{J K}^{-1} \text{mol}^{-1}) &= 1699.6822 - 3.6792X - 65.1883X^2 \\ &+ 376.8911X^3 + 1322.771X^4 - 301.2720X^5 \quad (2) \end{aligned}$$

where $X = (T - 388)/18$; $R^2 = 1.0000$. This equation is valid to the temperature range between 379 and 397 K.

3.2. The melting point, molar enthalpy and molar entropy of fusion

The melting temperature of the complex can be obtained from the C_p - T curve. The initial melting temperature is 363.64 K and the final melting temperature is 379.45 K. The phase transition temperature is 378.73 K. The sample coexists in two-phase states in the temperature range of 363.64–379.55 K. The molar enthalpy, ΔH_m , and molar entropy, ΔS_m , of the transition can be calculated based on the following equations:

$$\Delta H_m = \frac{Q - n \int_{T_i}^{T_m} C_{p,1} dT - n \int_{T_m}^{T_f} C_{p,2} dT - n \int_{T_i}^{T_f} H_0 dT}{n} \quad (3)$$

$$\Delta S_m = \frac{\Delta H_m}{T_m} \quad (4)$$

where T_i is a temperature slightly lower than the initial melting temperature, T_f a temperature slightly

Table 1

The experimental molar heat capacities of $[\text{Y}_2(\text{Ala})_4(\text{H}_2\text{O})_8](\text{ClO}_4)_6$ (molar mass: $M = 1274.88$)

T (K)	C_p ($\text{J K}^{-1} \text{mol}^{-1}$)	T (K)	C_p ($\text{J K}^{-1} \text{mol}^{-1}$)	T (K)	C_p ($\text{J K}^{-1} \text{mol}^{-1}$)
78.653	351.29	193.945	705.04	318.924	1396.52
80.530	351.86	197.269	717.66	321.788	1412.89
83.318	367.48	200.567	733.27	324.611	1439.64
86.024	370.59	203.844	740.08	327.384	1450.67
88.640	372.51	207.433	767.71	330.112	1468.27
91.212	373.40	211.347	804.80	332.794	1470.20
93.704	374.38	215.216	819.61	335.427	1472.39
96.143	375.33	219.043	827.62	338.010	1477.01
98.530	377.69	222.840	832.22	340.549	1485.05
101.249	383.00	226.587	848.83	343.039	1499.46
104.262	389.95	230.288	869.87	345.487	1521.21
107.196	397.41	234.010	876.76	347.896	1556.70
110.068	398.03	237.662	906.03	350.283	1560.79
112.885	400.98	241.232	924.95	352.622	1565.16
115.887	409.32	244.805	948.48	354.893	1574.97
119.040	417.42	248.377	958.72	357.127	1580.13
122.131	424.19	251.948	982.14	359.331	1577.40
125.173	434.53	255.438	1027.52	361.526	1586.65
128.162	441.16	258.929	1048.01	363.636	1595.43
131.386	445.67	262.338	1074.36	365.666	1620.32
134.821	453.75	265.747	1121.19	368.425	1728.63
138.149	462.53	269.156	1160.71	369.481	1898.42
141.477	469.85	272.484	1185.60	371.347	2284.84
144.793	480.36	275.812	1216.33	372.890	2634.66
148.026	494.44	279.058	1250.00	373.864	3028.40
151.531	507.83	282.305	1264.64	375.649	3444.09
155.295	541.48	285.552	1289.52	377.192	3871.49
159.006	555.11	288.718	1312.94	378.734	4483.31
162.671	572.99	291.802	1329.04	378.936	2513.17
166.286	590.38	294.886	1340.75	379.545	1661.30
169.863	606.01	297.971	1356.85	382.097	1683.26
173.407	617.68	300.974	1356.85	385.449	1697.89
176.908	630.20	304.058	1362.70	388.967	1699.36
180.372	655.49	307.143	1375.88	392.510	1700.82
183.817	659.96	310.101	1377.45	396.023	1718.38
187.220	678.82	313.071	1383.34		
190.597	692.03	316.010	1398.68		

higher than the final melting temperature, Q the total energy introduced into the sample cell from T_i to T_f , H_0 the heat capacity of the sample cell from T_i to T_f , $C_{p,1}$ the heat capacity of the sample in solid phase from T_i to T_m , $C_{p,2}$ the heat capacity of the sample in liquid phase from T_m to T_f and n is molar amount of the sample. The molar enthalpy and molar entropy of fusion of the sample were determined to be $16.78 \pm 0.02 \text{ kJ mol}^{-1}$ and $44.30 \pm 0.04 \text{ J K}^{-1} \text{mol}^{-1}$, respectively.

3.3. TG and DSC results

The DSC results are presented in Fig. 2, from which we can see that no thermal anomaly occurred below 80°C , which means that the structure of the complex, $[\text{Y}_2(\text{Ala})_4(\text{H}_2\text{O})_8](\text{ClO}_4)_6$ is stable below this temperature. However, an exothermic peak was observed at about 282.360°C .

The TG curve of $[\text{Y}_2(\text{Ala})_4(\text{H}_2\text{O})_8](\text{ClO}_4)_6$ are shown in Fig. 3. It can be seen clearly from the

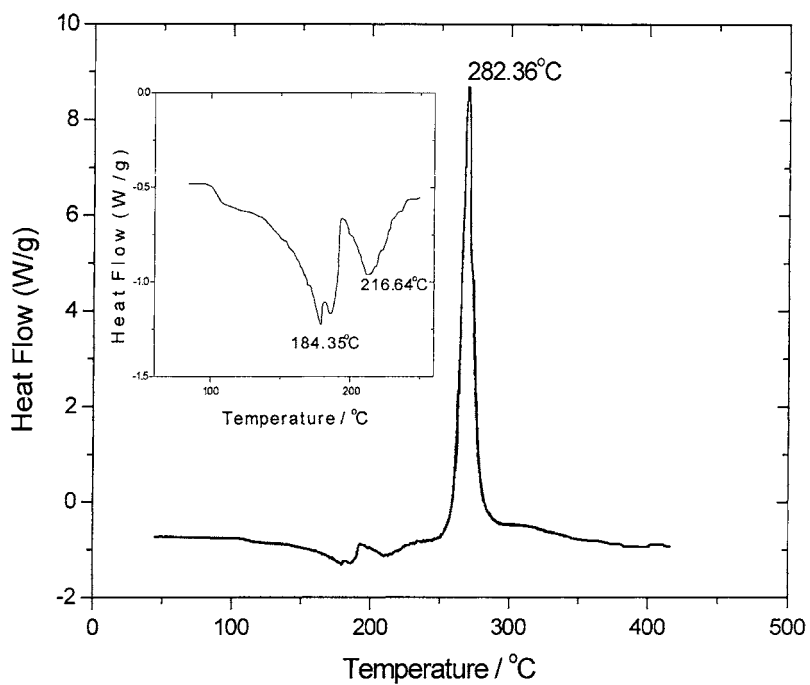


Fig. 2. DSC curve of $[Y_2(Ala)_4(H_2O)_8](ClO_4)_6$ under nitrogen atmosphere.

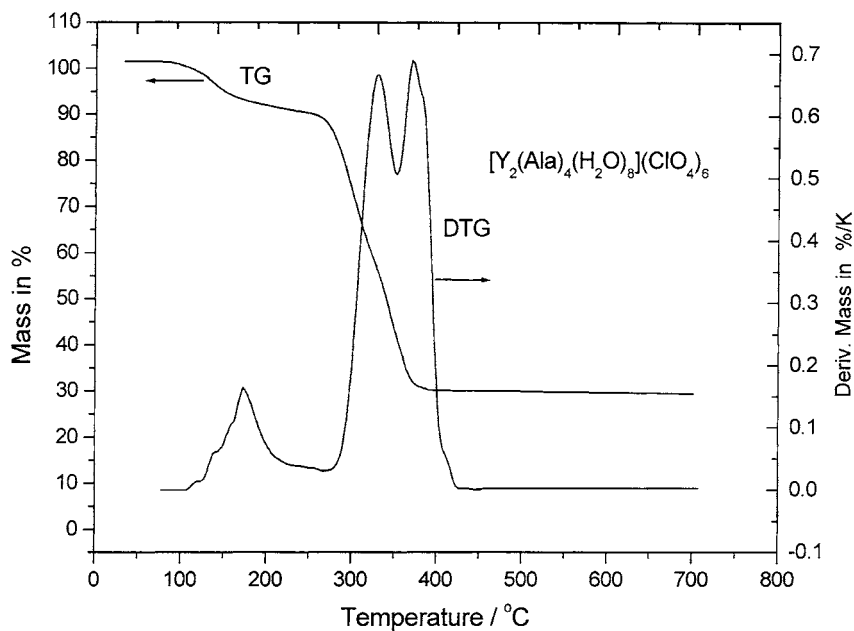
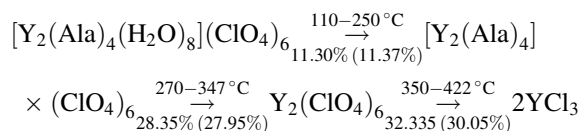


Fig. 3. TG curve of $[Y_2(Ala)_4(H_2O)_8](ClO_4)_6$ under nitrogen atmosphere.

mass-loss curve that the solid complex is very stable below 80 °C and started decomposition at this point, and the most mass-loss occurred in the temperature range of 250–350 °C. These accord well with the results obtained by DSC. The actual residue mass% is 32.33%. We consider that the residue should be YCl_3 , theoretically, because the corresponding residue mass% is 30.05% which is near to 32.33%. Possible mechanisms of the thermal decomposition may be deduced as following, according to the mass-loss in each step:



The mass-loss percentages in the brackets are the calculated theoretical values.

Acknowledgements

This work was financially supported by the National Nature Sciences Foundation of China (NSFC No.20073047).

References

- [1] J. Legendziewicz, *Inorg. Chim. Acta* 95 (1984) 57.
- [2] X.Y. Li, K.Z. Pan, *J. Struct. Chem.* 4 (1985) 56.
- [3] X.Y. Li, K.Z. Pan, *J. Struct. Chem.* 4 (1985) 75.
- [4] T.Z. Jin, S. Gao, C.H. Huang, Y.Z. Han, *Chinese Acta of Rare Earth Met.* 5 (1987) 3.
- [5] H.D. Zeng, K.Z. Pan, *J. Struct. Chem.* 11 (1992) 5.
- [6] B.S. Guo, *Rare Earth* 20 (1999) 64.
- [7] Z.C. Tan, G.Y. Sun, *J. Therm. Anal.* 45 (1995) 59.
- [8] D.A. Ditmars, S. Ishiara, S.S. Chang, G. Bernstein, E.D. West, *J. Res. Nat. Bur. Stand.* 87 (1982) 13.